Unusual Imaging Findings Associated with Germ Cell Tumors

Kirti Magudia, MD, PhD
Christine O. Menias, MD
Sanjeev Bhalla, MD
Venkata S. Katabathina, MD
Jeffrey W. Craig, MD, PhD
Mark M. Hammer, MD

Abbreviations: FDG = fluorine 18 fluorodeoxyglucose, FLAIR = fluid-attenuated inversion-recovery, H-E = hematoxylin-eosin, hCG = human chorionic gonadotropin, NMDA = *N*-methyl-D-aspartate

RadioGraphics 2019; 39:1019–1035

https://doi.org/10.1148/rg.2019180050

Content Codes: GU OB OI

From the Departments of Radiology (K.M., M.M.H.) and Pathology (J.W.C.), Brigham and Women's Hospital, 75 Francis St, Boston, MA 02115; Department of Radiology, Mayo Clinic Scottsdale, Scottsdale, Ariz (C.O.M.); Mallinckrodt Institute of Radiology, Washington University School of Medicine, St Louis, Mo (S.B.); and Department of Radiology, University of Texas Health Science Center, San Antonio, Tex (V.S.K.). Presented as an education exhibit at the 2017 RSNA Annual Meeting. Received March 4, 2018; revision requested June 13 and received July 11; accepted July 24. For this journal-based SA-CME activity, the authors, editor, and reviewers have disclosed no relevant relationships. **Address correspondence to** K.M. (e-mail: *kmagudia@bwh.harvard.edu*).

SA-CME LEARNING OBJECTIVES

After completing this journal-based SA-CME activity, participants will be able to:

- Recognize entities associated with germ cell tumors that may mimic worsening metastatic disease.
- Describe unusual manifestations of true metastatic disease that may occur in germ cell tumors.
- List systemic endocrine and autoimmune syndromes that may be caused by germ cell tumors.

See rsna.org/learning-center-rg.

Germ cell tumors, because they contain immature and mature elements, can differentiate into different tissue types. They can exhibit unusual imaging features or manifest in a syndromic fashion. The authors describe these features and assign them to one of the following categories: *(a)* unusual manifestations of metastatic disease (growing teratoma syndrome, choriocarcinoma syndrome, ossified metastases, and gliomatosis peritonei); *(b)* autoimmune manifestations (sarcoidlike reaction and paraneoplastic syndromes); *(c)* endocrine syndromes (sex hormone production, struma ovarii, and struma carcinoid); or *(d)* miscellaneous conditions (ruptured dermoid cyst, squamous cell carcinoma arising from a mature teratoma, Currarino triad, fetus in fetu, pseudo-Meigs syndrome, and pancreatitis). Rare conditions associated with germ cell tumors demonstrate characteristic imaging findings that can help lead to the appropriate diagnosis and management recommendations. When evaluating for potential metastatic disease, alternative benign diagnoses should be considered (eg, growing teratoma syndrome, ossified metastases, ruptured dermoid cyst, gliomatosis peritonei, and sarcoidlike reaction), which may impact management. Germ cell tumors may also lead to life-threatening complications such as extensive hemorrhage from choriocarcinoma metastases or the rupture of mature teratomas, cases in which timely diagnosis is crucial. Autoimmune and endocrine manifestations such as paraneoplastic encephalitis, autoimmune hemolytic anemia, and hyperthyroidism may occur owing to the presence of germ cell tumors and can create a diagnostic dilemma for clinicians. Knowledge of the syndromic and unusual imaging findings associated with germ cell tumors helps guide appropriate management.

Introduction

Germ cell tumors represent neoplasms derived from germ cells. These cells are normally found in the ovaries or testes, in which their function is to produce eggs or sperm, respectively. These gonadal sites are the most common locations for the manifestation of germ cell tumors. Germ cell tumors are also found in extragonadal sites, likely arising from primordial germ cells that fail to migrate to the gonads (1). Teratomas are a specific type of germ cell tumor that contain mature elements from all three embryonic germ layers—the ectoderm, mesoderm, and endoderm (1).

An earlier incorrect version of this article appeared online. This article was corrected on July 25, 2019.

TEACHING POINTS

- Growing teratoma syndrome is the growth of nonseminomatous germ cell tumor metastases, despite appropriate treatment with chemotherapy and the normalization of serum markers, with the results of a pathologic examination confirming mature teratoma.
- *Choriocarcinoma syndrome* is defined as extensive bleeding of choriocarcinoma metastases, which can lead to diffuse alveolar hemorrhage in the lungs and subcapsular hematoma in the liver.
- Because sarcoidlike reactions are associated with lymphadenopathy, they may mimic progression of metastatic disease.
- Many germ cell tumors will produce hCG, with associated downstream effects such as gynecomastia in men and virilization in women.
- A larger than expected soft-tissue component for an ovarian mature teratoma should raise concern for malignant transformation.

The classification of germ cell tumors is dependent on the site of manifestation (Fig 1). In the testicle, germ cell tumors are categorized as seminomatous or nonseminomatous (5). Seminomatous germ cell tumors are histologically pure seminoma and are more indolent and less likely to metastasize in comparison to those of nonseminomatous types (6,7). Nonseminomatous germ cell tumors may be comprised of a single cell type (eg, a yolk sac tumor) or a combination of several cell types, including seminoma (5).

In the ovary, germ cell tumors include mature teratoma (also known as dermoid cyst), immature teratoma, yolk sac tumor, mixed germ cell tumor, and choriocarcinoma, the latter of which includes gestational and nongestational forms (8,9). Note that testicular teratomas are classified as nonseminomatous germ cell tumors and are considered malignant, while mature teratomas of the ovary are considered benign (5,8).

Extragonadal germ cell tumors often develop in midline structures (Fig 1). In pediatric patients, extragonadal germ cell tumors are often found intracranially and in the pelvis, mediastinum, and retroperitoneum, from highest to lowest rate of prevalence, as well as in other sites (2,10). In adults, the most common sites of manifestation include the anterior mediastinum, retroperitoneum, and intracranial locations (3,4,9,11,12). Overall, extragonadal germ cell tumors in adults are extremely uncommon, composing 2% of all germ cell tumors. However, the prevalence of extragonadal tumors is higher in women (3).

Imaging plays a key role in the diagnosis and management of germ cell tumors. Primary gonadal tumors are most often depicted on US images, although CT or MRI can be performed for troubleshooting (13,14). In contrast, extragonadal tumors are most often depicted on CT or MR images (9). CT is also usually the modality of choice when staging germ cell tumors, although MRI may be preferred in younger patients owing to its lower radiation dose (13–15). Fluorine 18–fluorodeoxyglucose (FDG) PET/CT is not generally used to stage germ cell tumors, although PET/CT may provide value in the differentiation of viable versus nonviable tissue after therapy (13,15–17).

In this article, we review the unusual manifestations of germ cell tumors, including uncommon patterns of metastatic disease, autoimmune manifestations, associated endocrine syndromes, and miscellaneous syndromes and manifestations.

Unusual Manifestations of Metastatic Disease

Malignant germ cell tumors of the testes, ovaries, and retroperitoneum commonly metastasize to the retroperitoneal lymph nodes (14,18). The most common sites of solid-organ metastases from germ cell tumors are the lungs, followed by the liver and brain (13,14,19). Ovarian germ cell tumors may also spread directly to peritoneal surfaces (14). However, metastatic disease from germ cell tumors can occasionally have an unusual appearance or clinical presentation, and knowledge of these manifestations will allow the radiologist to interpret images correctly and provide the greatest value to referring clinicians.

Growing Teratoma Syndrome

Because of their totipotent nature, germ cell tumors have the capability of differentiating into various tissue types such as a teratoma. Rarely, metastases from nonseminomatous germ cell tumors can differentiate into mature teratomas after treatment with chemotherapy (20,21). These metastases are composed of benign cell types and are thus no longer susceptible to chemotherapy.

Growing teratoma syndrome is the growth of nonseminomatous germ cell tumor metastases, despite appropriate treatment with chemotherapy and the normalization of serum markers, with the results of a pathologic examination confirming mature teratoma. This enlargement may mimic treatment failure or relapse (21,22). This distinction is important for patient management as mature teratomas will not respond to further chemotherapy; they are often excised surgically (20). Growing teratoma syndrome more commonly manifests in men than in women (15).

The typical imaging findings of growing teratoma syndrome are enlargement and cystic change within existing metastases (Figs 2, 3)

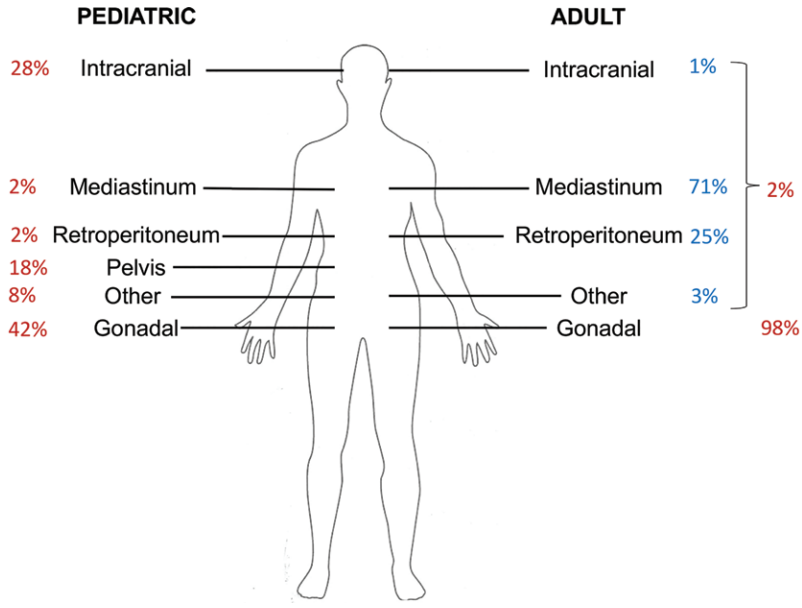

Figure 1. Frequency of germ cell tumors in pediatric and adult patients by site of manifestation. Illustration shows the overall distribution of germ cell tumors in pediatric and adult patients (red percentages). The 2% of extragonadal tumors diagnosed in adults is further categorized by location (blue percentages). (Data are from references 2–4.)

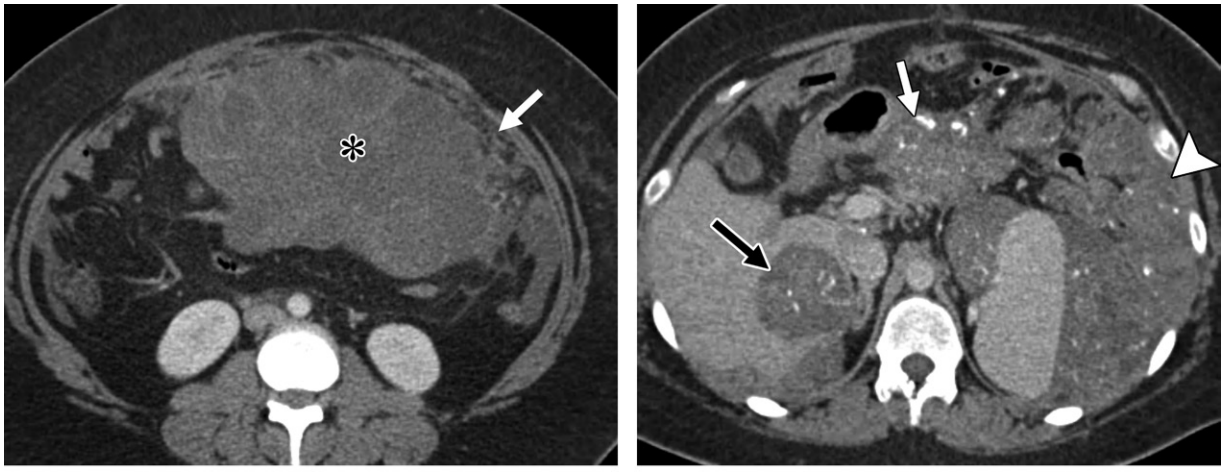

a. **b.**

Figure 2. Growing teratoma syndrome in a 27-year-old woman with an ovarian mixed germ cell tumor treated with resection and chemotherapy. **(a)** Axial contrast material–enhanced CT image obtained before treatment shows a mixed solid and cystic intraperitoneal mass (*), with surrounding peritoneal fat stranding and nodularity (arrow). **(b)** Axial contrast-enhanced CT image obtained after treatment shows hepatic (black arrow), mesenteric (white arrow), and peritoneal (arrowhead) mixed cystic and solid lesions with internal calcification. Surgical resection confirmed mature teratomas.

(21,23). Growing teratomas may also calcify (Fig 2), a finding that represents the presence of mature osseous and cartilaginous elements within the teratoma, and develop intralesional fat (24). These enlarging masses generally show minimal contrast enhancement, often at the rim or septa rather than nodular enhancement (Fig 3c).

MRI may be helpful in distinguishing proteinaceous material from true enhancement and for better delineating the relationship between the tumor and adjacent structures. PET/CT images will show minimal or no residual FDG uptake (Fig 3b, 3d) (21). Dual-energy CT images can also show lack of enhancement within these lesions. If a radiologist is confronted with a case of nonseminomatous germ cell tumor metastases with enlarging cystic non–FDG-avid lesions despite an otherwise good response to therapy, he or she should suspect a diagnosis of growing teratoma syndrome.

Choriocarcinoma Syndrome

Choriocarcinoma produces hypervascular metastases, which promote angiogenesis and

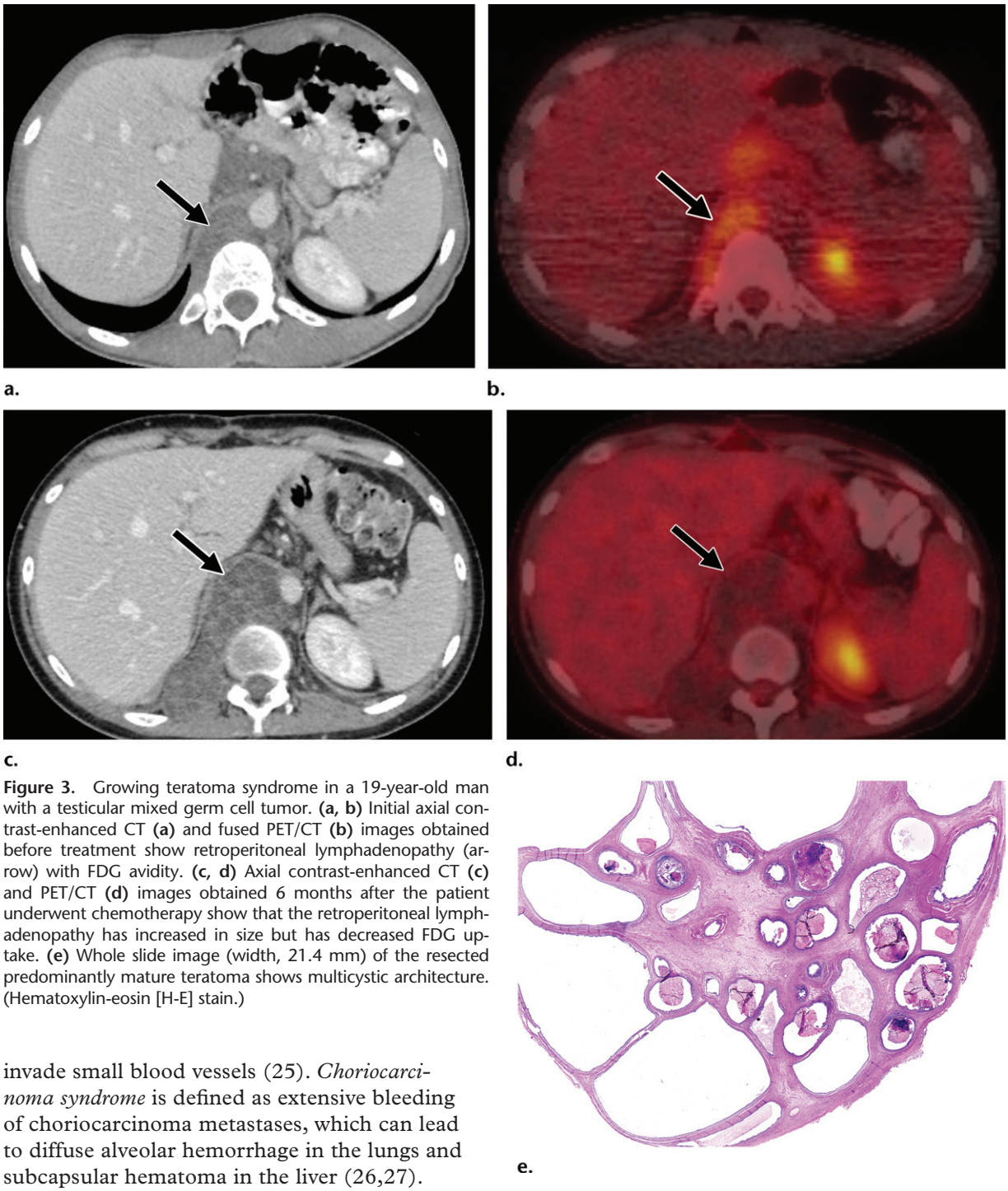

Figure 3. Growing teratoma syndrome in a 19-year-old man with a testicular mixed germ cell tumor. **(a, b)** Initial axial contrast-enhanced CT **(a)** and fused PET/CT **(b)** images obtained before treatment show retroperitoneal lymphadenopathy (arrow) with FDG avidity. **(c, d)** Axial contrast-enhanced CT **(c)** and PET/CT **(d)** images obtained 6 months after the patient underwent chemotherapy show that the retroperitoneal lymphadenopathy has increased in size but has decreased FDG uptake. **(e)** Whole slide image (width, 21.4 mm) of the resected predominantly mature teratoma shows multicystic architecture. (Hematoxylin-eosin [H-E] stain.)

invade small blood vessels (25). *Choriocarcinoma syndrome* is defined as extensive bleeding of choriocarcinoma metastases, which can lead to diffuse alveolar hemorrhage in the lungs and subcapsular hematoma in the liver (26,27). Severe cases of choriocarcinoma syndrome may result in disseminated intravascular coagulation, massive hemorrhage, and shock (25–28).

This syndrome is more commonly seen in patients with a large disease burden or immediately after initiating chemotherapy (29,30). Usually, choriocarcinoma syndrome is associated with markedly elevated human chorionic gonadotropin (hCG) levels (30). This syndrome is associated with poor response to therapy and poor outcomes (26,27,30).

The typical imaging findings associated with choriocarcinoma syndrome are dependent on the site of metastasis. In the lungs, metastatic nodules have surrounding ground-glass attenuation (CT halo sign), a finding consistent with hemorrhage. As bleeding becomes more extensive, patchy ground-glass opacities may be depicted throughout the lung, a finding consistent with diffuse alveolar hemorrhage (25,26,29). Hemothorax has also been reported (28). In the liver, hemorrhagic metastases can lead to subcapsular hematoma and hemoperitoneum (Fig 4a) (27).

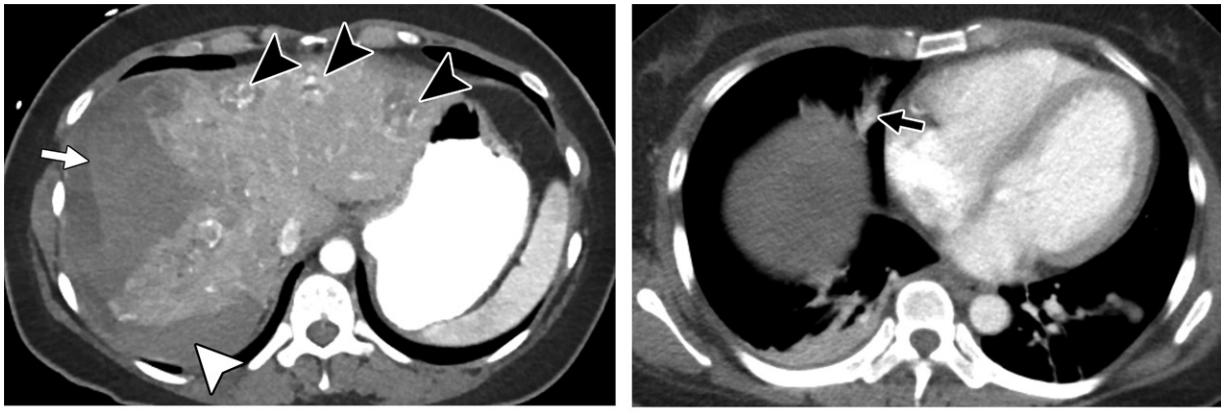

a. b.

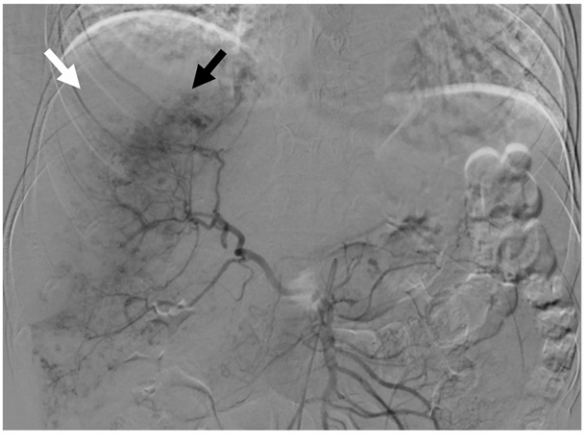

c.

Figure 4. Choriocarcinoma syndrome in a 35-year-old woman who presented with abdominal pain. Laboratory findings disclosed anemia and an elevated hCG level without intrauterine pregnancy. **(a, b)** Axial contrast-enhanced CT images show multiple pseudoaneurysms in the liver (black arrowheads in **a**), subcapsular hematoma in the liver (arrow in **a**), and hyperattenuating ascites (white arrowhead in **a**). A pseudoaneurysm in the middle lobe of the right lung (arrow in **b**) is also depicted. **(c)** Selective digital subtraction angiogram of the superior mesenteric artery shows tumor vascularity (black arrow) in the liver. Paucity of vascularity (white arrow) is also depicted at the site of the subcapsular hematoma. The results of pathologic analysis of a liver biopsy specimen confirmed metastatic choriocarcinoma.

In some cases, metastases may produce pseudoaneurysms or arteriovenous fistulas (Fig 4a, 4b) (28,30). Catheter angiograms will depict tumor vascularity and, in some cases, pseudoaneurysms that may require urgent catheter-directed embolization to manage associated hemorrhage (Fig 4c). In the absence of a known diagnosis of metastatic choriocarcinoma, the differential diagnosis for multiple pseudoaneurysms and/or hemorrhagic masses would include hypervascular metastases from choriocarcinoma, renal cell carcinoma, thyroid carcinoma, angiosarcoma, or hemangioendothelioma.

Ossified Metastases

Ossified metastases in the lungs are rare and usually associated with metastatic osteosarcoma (31). Although unreported, ossified metastases may also be diagnosed in a patient with a malignant germ cell tumor. For example, the patient in Figure 5 was diagnosed initially with a mediastinal immature teratoma and soft-tissue–attenuation pulmonary nodules. After treatment, the pulmonary nodules increased in size and developed calcification at CT (Fig 5b). The results of a pathologic examination of one of the excised lung nodules confirmed mature osseous tissue (Fig 5c). We hypothesize that metastatic teratoma in the lung differentiated into mature osseous tissue, analogous to growing teratoma syndrome.

In general, radiologists should consider calcifying granulomas and calcifying metastases in the differential diagnosis for a calcifying pulmonary nodule depicted in the setting of a known malignancy. Performing a biopsy may be required for confirmation.

Gliomatosis Peritonei

Another uncommon path of differentiation for immature germ cell tumors is glial tissue. In patients with immature teratoma of the ovary, tumor cells can seed the peritoneum and differentiate into glia (32). The glial tissue is usually benign, although transformation to malignant glioma has been described (33). Gliomatosis peritonei usually manifests in the pediatric to middle-aged adult population and is not associated with poor prognosis.

An imaging feature of gliomatosis peritonei is nodular enhancement of the peritoneum, which cannot be distinguished from conventional metastases by imaging alone (Fig 6) (32). Of note, gliomatosis peritonei can also rarely result from peritoneal seeding of the intracranial glial tissue through a ventriculoperitoneal shunt (33).

Autoimmune Manifestations

Like many other malignancies, germ cell tumors can elicit an immune reaction that may affect

Figure 5. Ossified metastases in a 51-year-old man with mediastinal teratoma. **(a)** Initial axial contrast-enhanced CT image shows a small pulmonary metastasis (arrow). **(b)** Axial contrast-enhanced CT image obtained 8 months later shows the nodule (arrow), which has increased in size and developed calcification. **(c)** Photomicrograph (width, 3.5 mm) of the ossified pulmonary nodule shows lung tissue (arrowhead) with a large deposit of mature bone (arrow). (H-E stain; original magnification, ×40.)

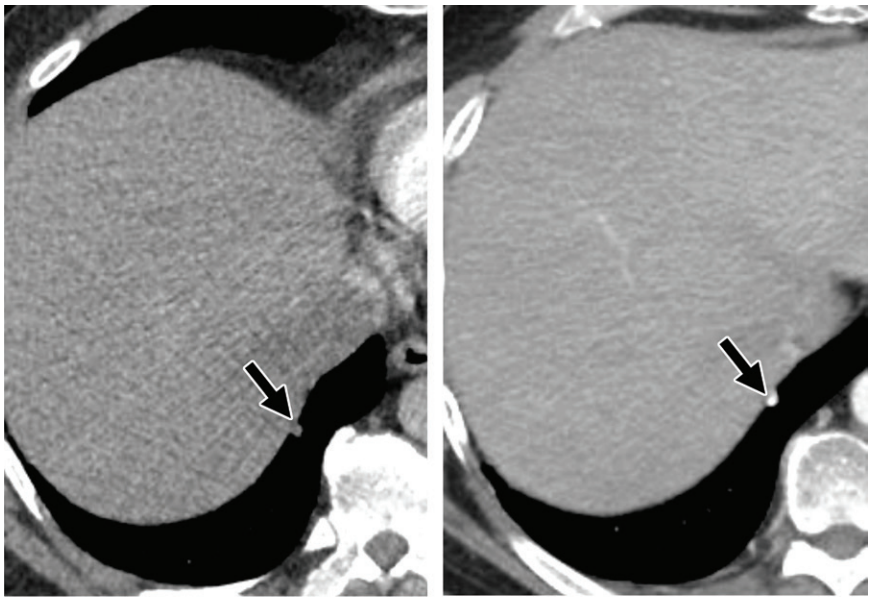

a. b.

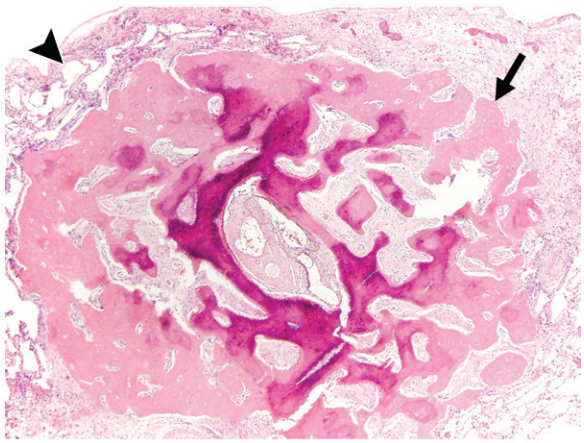

c.

normal organs. These immune reactions include sarcoidlike reaction, granulomatous inflammation that pathologically mimics sarcoidosis, and various paraneoplastic syndromes, particularly with neurologic manifestations.

Sarcoidlike Reaction

Sarcoidosis is a systemic inflammatory process characterized by nonnecrotizing granulomatous inflammation. It can affect multiple organs, particularly the eyes, lymph nodes, lungs, central nervous system, and heart. A sarcoidlike reaction represents a granulomatous inflammatory process that occurs in the setting of malignancy or infection but does not meet the clinical criteria of sarcoidosis (34).

The pathogenesis of sarcoidlike reaction is unknown but hypothesized to be caused by humoral and T-cell–mediated factors, leading to the recruitment and activation of macrophages (35). Sarcoidlike reactions are not typically associated with symptoms and rarely require treatment. Because sarcoidlike reactions are associated with lymphadenopathy, they may mimic the progression of metastatic disease.

Indeed, a study of sarcoidlike reactions in a general oncology population reported that sarcoidlike reaction was pathologically confirmed in 0.6% of the oncology population undergoing PET/CT, more frequently at restaging compared with at initial staging. Astute recognition of possible sarcoidlike reactions may prevent incorrect staging and management of this population, as sarcoidlike reaction is treated conservatively or with steroids rather than with chemotherapy (35). However, the results of a biopsy are usually required to obtain a definitive diagnosis (36). Sarcoidlike reactions have been reported in association with germ cell tumors both before and after treatment (36).

The typical imaging appearance of sarcoidlike reaction includes mediastinal and hilar lymphadenopathy, which may form the Garland triad, also termed the *1-2-3 sign* or *pawnbroker sign,* on chest radiographs, corresponding to the right paratracheal and bilateral hilar stations (Figs 7a, 8b) (36,37). Less commonly, perilymphatic

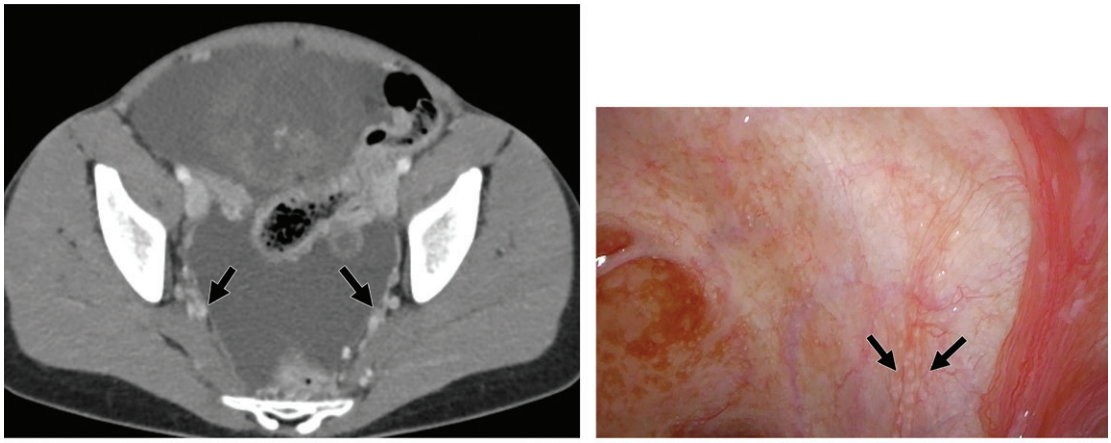

a. b.

Figure 6. Gliomatosis peritonei in a 12-year-old girl with a history of immature teratoma following resection. **(a)** Axial contrast-enhanced CT image shows ascites with nodular enhancement of the peritoneum (arrows). **(b)** Laparoscopic image shows studding of the peritoneum (arrows). The results of a pathologic examination confirmed gliomatosis peritonei.

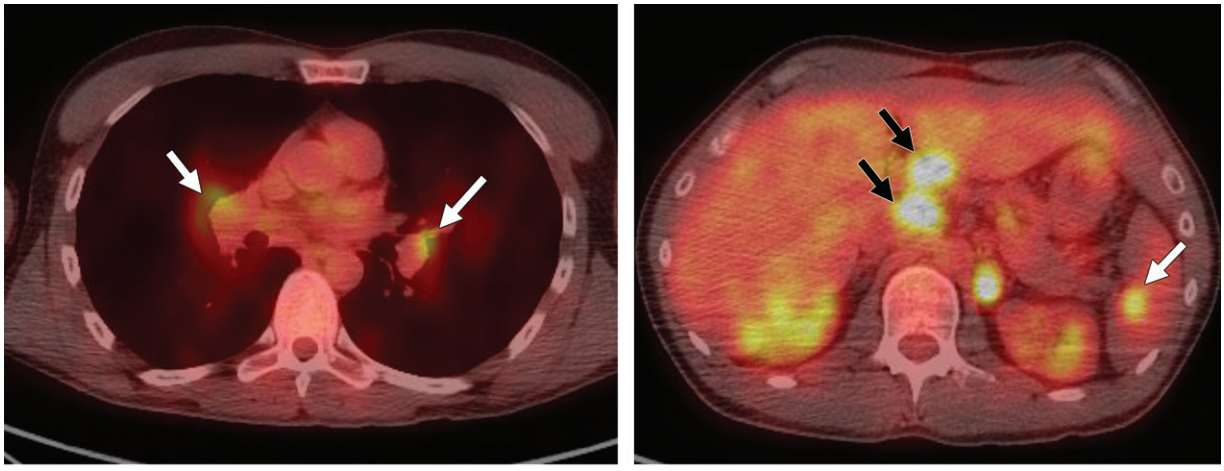

a. c.

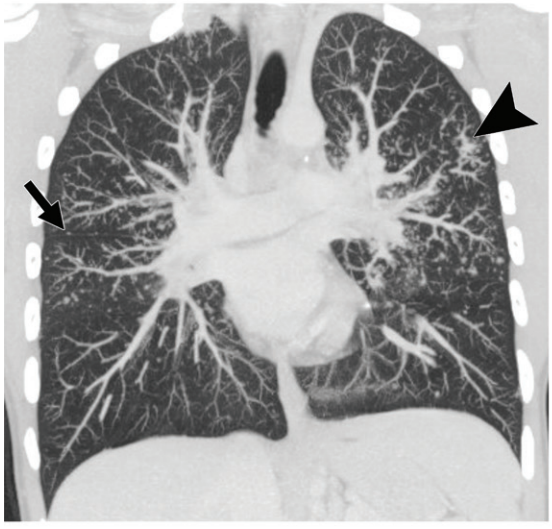

b.

Figure 7. Sarcoidlike reaction in a 41-year-old man with testicular teratoma who underwent treatment 18 years earlier and was diagnosed with pelvic recurrence. **(a)** Axial fused PET/CT image shows FDG-avid hilar lymphadenopathy (arrows). **(b)** Coronal maximum intensity projection CT image of the chest shows extensive diffuse perilymphatic pulmonary nodules with an upper lung predominance. Note the nodularity along the right minor fissure (arrow) and clustered nodules in the left upper lobe (arrowhead). **(c)** Axial fused PET/CT image shows FDG-avid upper abdominal lymphadenopathy (black arrows) and focal FDG uptake in the spleen (white arrow). The results of a pathologic examination confirmed granulomatous inflammation.

pulmonary nodules (Fig 7b) may manifest. Other sites such as the spleen and supraclavicular or upper abdominal lymph nodes can also be involved (Figs 7c, 8a) (36).

As both sarcoidlike reaction and metastatic disease show FDG uptake at imaging, PET/CT is not helpful in differentiating between these entities (Fig 7a, 7c) (35,36). Thus, when evaluating a staging examination for a patient with a known germ cell tumor, if the radiologist observes isolated hilar and paratracheal lymphadenopathy and/or perilymphatic pulmonary nodules, he or she should suggest that these represent a sarcoidlike reaction, as this would be an unusual distribution for metastases.

Figure 8. Sarcoidlike reaction in a 51-year-old woman. Axial nonenhanced CT images show a right supraclavicular lymphadenopathy (arrow in **a**), anterior mediastinal mass (* in **b**), pulmonary nodule (arrow in **b**), and right paratracheal lymphadenopathy (arrowhead in **b**). The supraclavicular lymph node was initially suspected to be metastatic, but the results of a biopsy confirmed granulomatous inflammation. The results from a pathologic examination of the anterior mediastinal resected mass confirmed choriocarcinoma, and the results of a surgical lung biopsy confirmed metastatic choriocarcinoma.

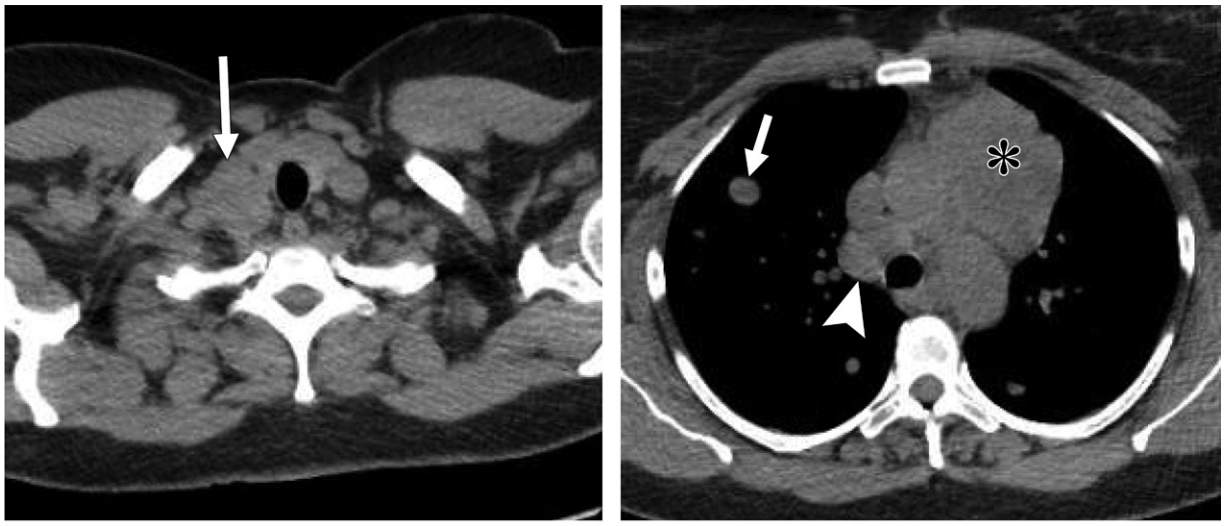

a. **b.**

Antibody-mediated Paraneoplastic Syndromes

Tumors may induce the patient's immune system to produce antibodies that harm normal tissues within the body. These are referred to as *paraneoplastic syndromes* and can involve various organ systems. Testicular germ cell tumors are associated with anti-Ma2 antibody–mediated encephalitis, in which patients present with memory loss, sleep disturbances, and hyperphagia and are diagnosed with pituitary hormone deficiencies (38). Ovarian teratomas are associated with anti–*N*-methyl-D-aspartate (NMDA)–receptor antibody–mediated encephalitis, which may cause patients to present with psychiatric symptoms and may lead to a catatonic state.

In both syndromes, paraneoplastic encephalitis is often the initial manifestation, and the occult primary tumor is identified at subsequent workup (39). Paraneoplastic encephalitis may be entirely occult at imaging, including at brain MRI. If depicted, the typical imaging features on MR images include a T2-weighted and/or fluid-attenuated inversion-recovery (FLAIR) signal intensity abnormality in the medial temporal lobes, cerebral cortex, or basal ganglia, usually without abnormal enhancement (Fig 9) (38,40,41). Paraneoplastic syndrome typically resolves after tumor resection and treatment with immunosuppression and intravenous immunoglobulin therapies (39).

Ovarian teratomas are rarely associated with autoimmune hemolytic anemia. The mechanism is unknown but likely relates to cross reactivity between tumor antigens and red blood cell surface antigens. The few reported cases of autoimmune hemolytic anemia are associated with splenomegaly. This entity does not respond to steroids or splenectomy but resolves when the teratoma is resected (42).

Endocrine Syndromes

Germ cell tumors may secrete hormones into the bloodstream, leading to downstream endocrine effects. These hormones may also aid in diagnosis and tumor monitoring.

Human Chorionic Gonadotropin

Many germ cell tumors will produce hCG, with associated downstream effects such as gynecomastia in men and virilization in women. Levels of hCG are elevated in 10%–20% of stage 1 cases and up to 40% of stage 2 cases of nonseminomatous germ cell tumors owing to the presence of embryonal carcinoma and/or choriocarcinoma elements (43). Even pure seminomas may produce hCG, which is seen in 15%–20% of patients with advanced seminomas owing to the presence of syncytiotrophoblasts (43,44). Elevated hCG levels are considered a poor prognostic factor in tumor staging (6).

In ovarian germ cell tumors, hCG levels are elevated in all choriocarcinomas and 5% of dysgerminomas; hCG may be produced in mixed germ cell tumors depending on their histologic composition (45). Elevated hCG levels have also been described in a case of ovarian mature teratoma (46).

Figure 9. Limbic encephalitis in a 22-year-old woman with a mature ovarian teratoma who presented with seizure. **(a, b)** Axial FLAIR MR images of the brain show increased signal intensity in the anteromedial bilateral frontal lobes (arrowhead in **a**), medial parietal lobes (arrow in **a**), and left thalamus (arrow in **b**). **(c)** Axial T1-weighted MR image of the pelvis shows a right adnexal mass (arrow) containing internal fat (*). The results of a pathologic examination of the right adnexal mass confirmed a mature ovarian teratoma. The patient was clinically diagnosed with anti–NMDA-receptor antibody–mediated encephalitis, with clinical improvement after mass resection and intravenous immunoglobulin therapy.

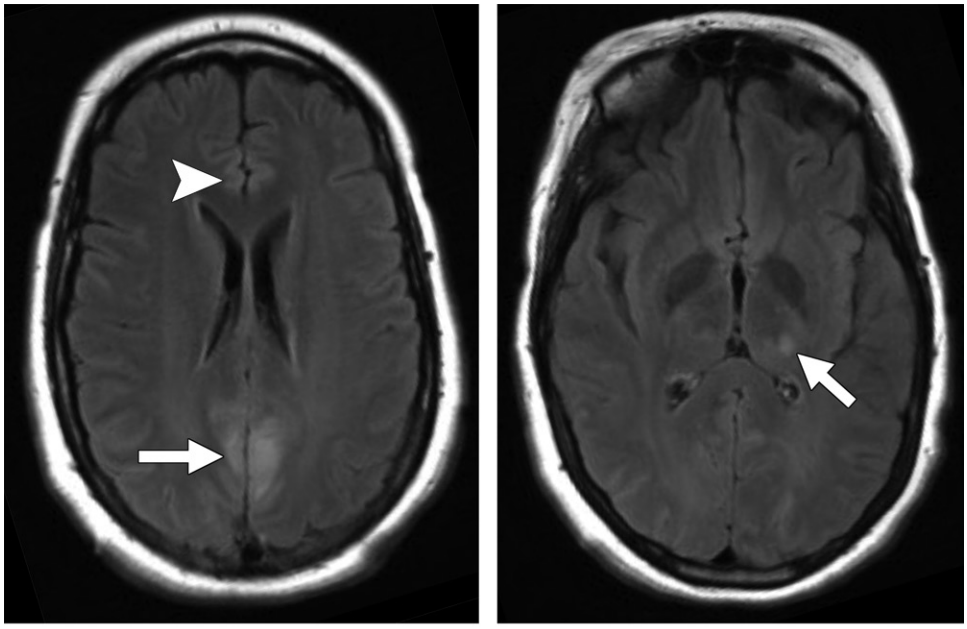

a. **b.**

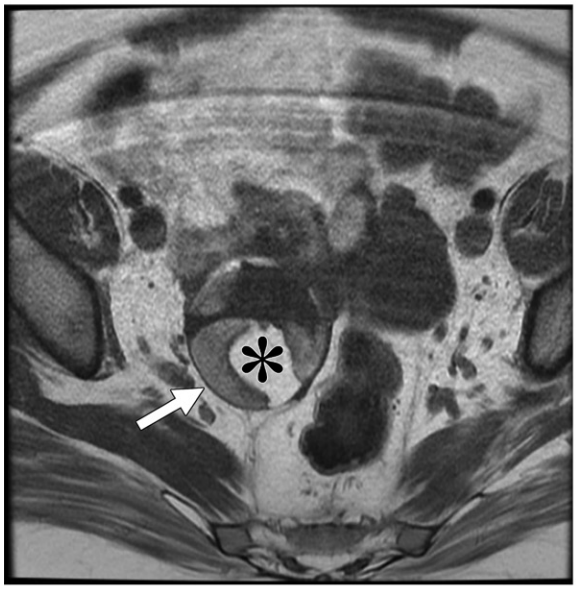

c.

Germ cell tumors produce a complete hCG molecule, which will then stimulate sex hormone production. In prepubertal patients, these elevated sex hormone levels result in precocious puberty (47). In male patients, elevated sex hormone levels may lead to gynecomastia and nipple soreness (Fig 10) (15,30). Gynecomastia typically appears as a flame-shaped or fan-shaped retroareolar lesion at mammography, a hypoechoic retroareolar mass at US, and a flame-shaped retroareolar soft-tissue lesion at CT (48). In female patients, elevated sex hormone production leads to primary or secondary amenorrhea and virilization, which includes symptoms such as hirsutism, acne, clitoromegaly, and voice changes (15,45).

Extreme elevation of hCG above 50 000 IU/L can stimulate thyroid hormone production, as the hCG hormone is similar in molecular structure to that of the thyroid-stimulating hormone (27,49). Patients with elevated hCG levels may be diagnosed with clinical hyperthyroidism and enlargement of the thyroid at imaging (49).

Thyroid and Carcinoid Differentiation

As discussed previously, teratomas contain mature tissues derived from the three germ layers within them. Struma ovarii and strumal carcinoid are ovarian teratomas that contain mature thyroid tissue and carcinoid tissue, respectively. To meet the criteria for a struma ovarii diagnosis, an ovarian teratoma must be composed of greater than 50% thyroid tissue (50). Strumal carcinoid refers to a rare ovarian teratoma composed of an admixture of carcinoid and thyroid tissue (51). Patients with either struma ovarii or strumal carcinoid can be diagnosed with clinical hyperthyroidism that resolves when the tumors are excised. Struma ovarii have been reported to occur in 2.7% of cases of all ovarian teratomas and 0.5% of all cases of ovarian malignant tumors,

Figure 10. Testicular teratoma in a 25-year-old man with an elevated serum β-hCG level of 1200 IU/L. Axial contrast-enhanced CT image shows bilateral gynecomastia (arrows).

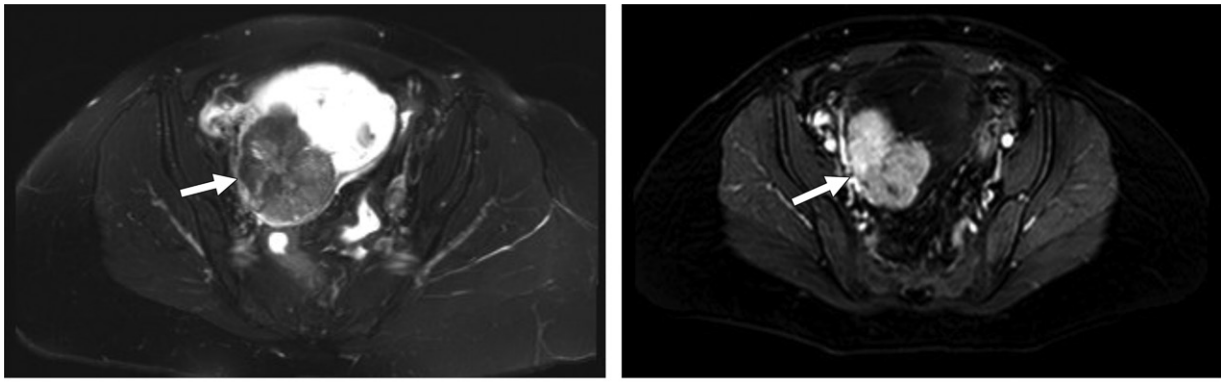

a. **b.**

Figure 11. Strumal carcinoid in a 53-year-old woman. **(a)** Axial T2-weighted fat-saturated MR image shows a T2-intermediate right adnexal mass (arrow). **(b)** Axial T1-weighted fat-saturated MR image obtained after the administration of contrast material (postcontrast) shows avid enhancement of the mass (arrow). The results of a pathologic examination confirmed strumal carcinoid.

with 5% of these patients diagnosed with clinical hyperthyroidism (14).

Struma ovarii and strumal carcinoid cannot be distinguished from other ovarian teratomas on the basis of conventional imaging. Struma ovarii will typically appear as a multilocular cystic mass on CT and MR images, often with enhancing septa and smooth margins. Large cystic spaces may occasionally be depicted, which represent dilated thyroid follicles (14).

Given the nonspecific imaging features, the diagnosis is usually made pathologically after resection. Struma ovarii and strumal carcinoid can also be incidentally detected on radioiodine images or explain low thyroid radioiodine uptake owing to the presence of ectopic thyroid tissue (52,53) (Fig 11). Papillary thyroid carcinoma will develop in an estimated 5% of patients with struma ovarii tumors. Typical management is staging and treatment with iodine-131 therapy after resection (50,52,53).

Miscellaneous Syndromes and Manifestations

Unusual imaging findings may suggest specific types of germ cell tumors. Knowledge of these syndromes and manifestations will allow radiologists to provide more specific diagnoses to aid clinical management.

Ruptured Dermoid Cyst

Mature ovarian teratomas or dermoid cysts may come to the clinician's attention in several ways. They are commonly visualized incidentally at CT or US performed for another indication. Patients may be diagnosed with ovarian torsion, characterized on US images as an enlarged ovary with decreased internal vascularity in the presence of a fat-containing mass, findings consistent with an ovarian mature teratoma. Similar findings are depicted at CT and MRI, which may also demonstrate medialization of the affected ovary (54,55).

Although uncommon, dermoid cysts may freely rupture into the peritoneal cavity. This may be spontaneous or occur after trauma, ovarian torsion, infection, or labor. These patients may be diagnosed acutely with peritonitis related to bleeding and the spilling of the teratoma's contents (56). This acute presentation can be associated with pain and anemia and may lead to hemorrhagic shock in some cases.

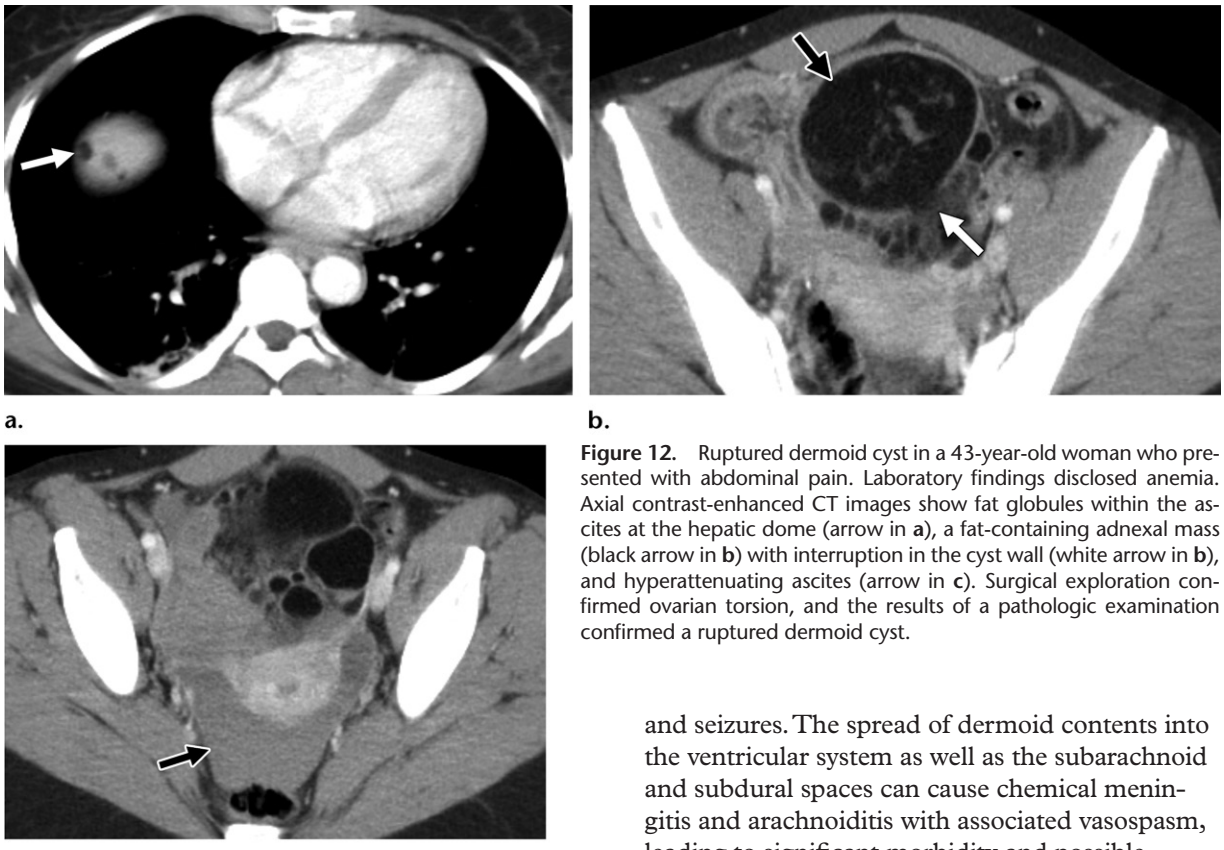

Figure 12. Ruptured dermoid cyst in a 43-year-old woman who presented with abdominal pain. Laboratory findings disclosed anemia. Axial contrast-enhanced CT images show fat globules within the ascites at the hepatic dome (arrow in **a**), a fat-containing adnexal mass (black arrow in **b**) with interruption in the cyst wall (white arrow in **b**), and hyperattenuating ascites (arrow in **c**). Surgical exploration confirmed ovarian torsion, and the results of a pathologic examination confirmed a ruptured dermoid cyst.

CT images will depict hemoperitoneum and occasionally free intraperitoneal fat globules (Fig 12) (54). Fat globules may be more difficult to visualize on MR images, as both fat and water are T2 hyperintense with fast spin-echo T2-weighted sequences. If fat globules floating within the peritoneal fluid are depicted, the radiologist should evaluate for an ovarian mass and suggest the diagnosis of ruptured dermoid cyst.

An alternate presentation of a ruptured dermoid cyst is chronic granulomatous peritonitis owing to a long-standing leaking teratoma (56). Typical imaging features of chronic granulomatous peritonitis include ascites and peritoneal enhancement, findings similar to those of peritoneal carcinomatosis or tuberculous peritonitis (54).

Teratomas from primary sites other than the ovary can rupture as well, including within the mediastinum and cranium. Several cases of ruptured mediastinal teratoma have been reported. This rupture may be spontaneous and is associated with chest pain, dyspnea, or hemoptysis (57–61). One case of mediastinal teratoma with rupture owing to trauma has also been reported (62). CT can show fat-containing pulmonary masses, pleural effusions, or pericardial effusion, and there may be consequent atelectasis or consolidation (58).

Intracranial dermoid cysts can also rupture and usually cause patients to present with headache and seizures. The spread of dermoid contents into the ventricular system as well as the subarachnoid and subdural spaces can cause chemical meningitis and arachnoiditis with associated vasospasm, leading to significant morbidity and possible mortality. Chemical meningitis leads to intense meningeal enhancement on MR images.

Similar to those depicted in the rupture of an ovarian mature teratoma, fat droplets may be visualized at both CT and MRI in the ventricular and subarachnoid spaces (63). Note that fat may be mistaken for air on standard brain-window CT images, so if a ruptured dermoid cyst is suspected, we suggest using standard soft-tissue (abdomen) windows. As discussed previously, both fat and cerebrospinal fluid will be hyperintense at T2-weighted MRI. T1-weighted MRI without fat suppression will readily demonstrate intracranial fat droplets.

Squamous Cell Carcinoma Arising from a Mature Teratoma

Mature teratomas may rarely undergo malignant transformation. Any component of the mature teratoma may become malignant, with squamous cell carcinoma representing the most frequent malignancy (64,65). Degeneration to adenocarcinoma or melanoma has also been reported (65).

Malignant transformation occurs in up to 2% of ovarian teratomas and is diagnosed more often in older patients. This diagnosis is associated with poor prognosis compared with mature teratoma alone and has treatment implications (65). Malignant transformation to squamous cell carcinoma may be associated with elevated

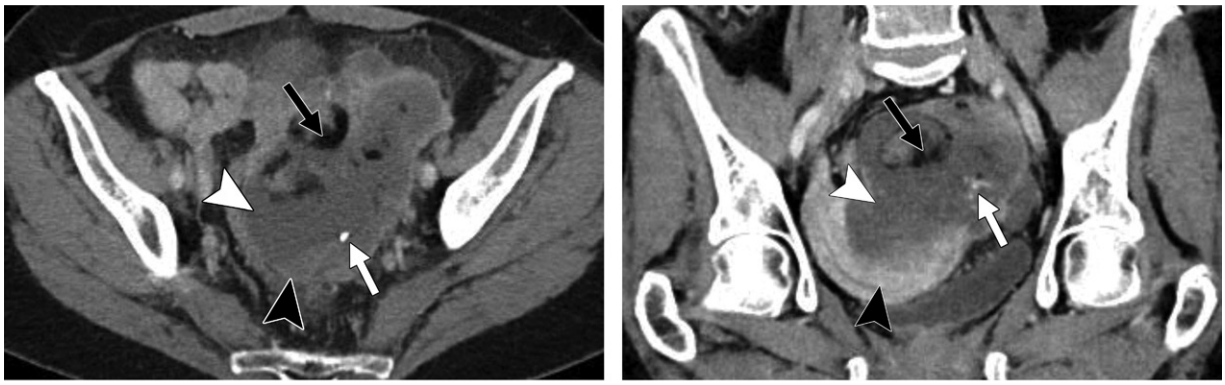

a. b.

Figure 13. Squamous cell carcinoma arising from a mature teratoma in a 57-year-old woman. Axial **(a)** and coronal **(b)** contrast-enhanced CT images show a large adnexal mass containing fat (black arrow), calcium (white arrow), fluid (white arrowhead), and a significant soft-tissue component (black arrowhead, better depicted on **b**). The results of a pathologic examination confirmed squamous cell carcinoma arising within a mature teratoma.

Figure 14. Immature teratoma in a 12-year-old girl. **(a)** Coronal contrast-enhanced CT image shows a large mass arising from the pelvis, predominately composed of heterogeneous soft tissue (white arrow), with small foci of calcium (black arrow) and fat (arrowhead). **(b)** Gross photograph of the resected mass shows heterogeneity with multiple tissue types. The results of a pathologic examination confirmed immature teratoma.

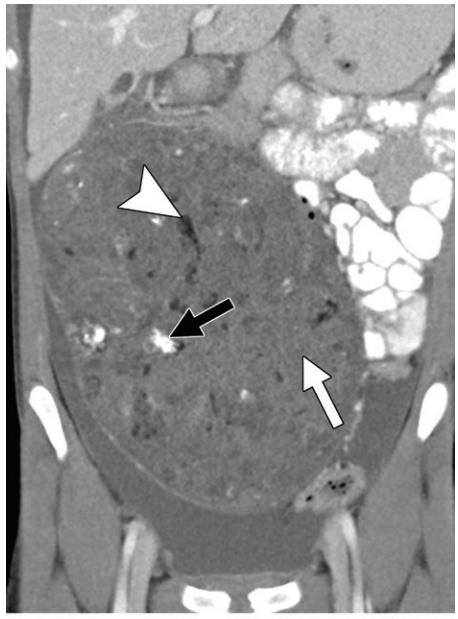

a.

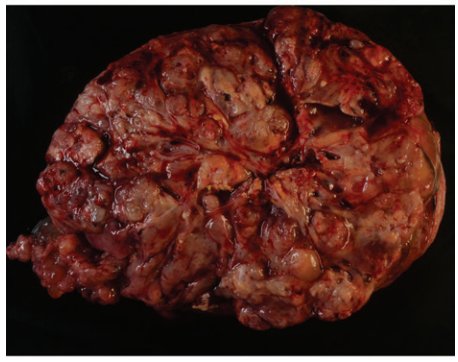

b.

carbohydrate antigen 19–9 or squamous cell carcinoma antigen levels (65,66). It has been suggested that teratomas in older patients or patients with large teratomas be screened for these tumor markers (66).

Preoperative diagnosis of the presence of squamous cell carcinoma within a mature teratoma is extremely challenging, as there are no imaging features specific for malignant degeneration. A larger than expected soft-tissue component for an ovarian mature teratoma should raise concern for malignant transformation (Fig 13). However, a large soft-tissue component within a teratoma can represent either malignant degeneration of mature elements (eg, carcinoma, which usually occurs in older patients) or malignancy within immature elements (eg, immature teratoma, which usually occurs in younger patients) (Fig 14) (1,64).

The degree of FDG uptake at PET/CT may also assist in differentiating mature teratomas from immature teratomas or teratomas with malignant transformation (67,68). Aggressive features such as invasion of adjacent structures should also suggest malignant potential (Fig 15). Indeed, one case series showed that 34% of teratomas with malignant degeneration to squamous cell carcinoma showed vascular involvement, and 67% showed infiltration of surrounding structures at pathologic examination (65). MRI can be helpful in distinguishing proteinaceous material from enhancing soft tissue and delineating any invasion of adjacent structures. Rapid growth may also be suggestive of malignant transformation (64).

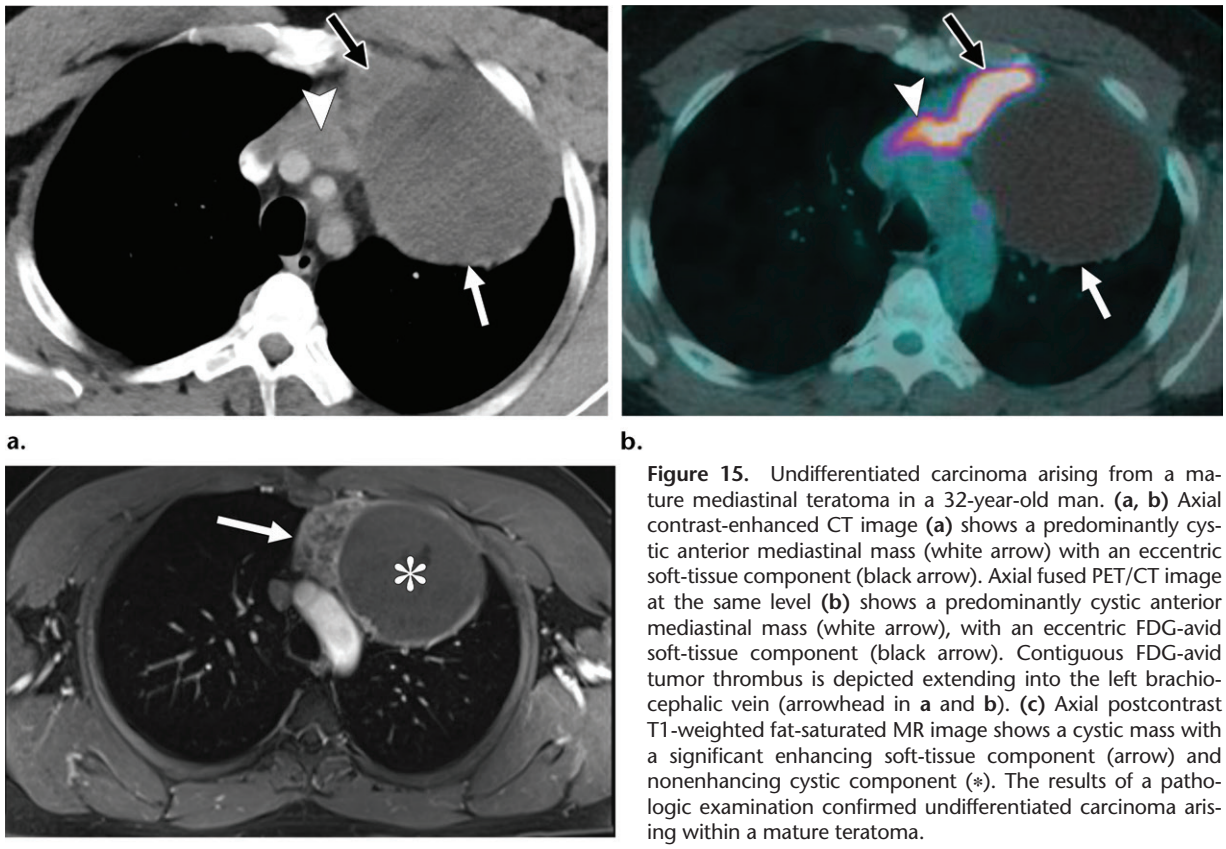

Figure 15. Undifferentiated carcinoma arising from a mature mediastinal teratoma in a 32-year-old man. **(a, b)** Axial contrast-enhanced CT image **(a)** shows a predominantly cystic anterior mediastinal mass (white arrow) with an eccentric soft-tissue component (black arrow). Axial fused PET/CT image at the same level **(b)** shows a predominantly cystic anterior mediastinal mass (white arrow), with an eccentric FDG-avid soft-tissue component (black arrow). Contiguous FDG-avid tumor thrombus is depicted extending into the left brachiocephalic vein (arrowhead in **a** and **b**). **(c)** Axial postcontrast T1-weighted fat-saturated MR image shows a cystic mass with a significant enhancing soft-tissue component (arrow) and nonenhancing cystic component (*). The results of a pathologic examination confirmed undifferentiated carcinoma arising within a mature teratoma.

Currarino Triad

Currarino triad represents the association of a presacral mass, sacral osseous defect, and anorectal malformation in pediatric patients (69). Patients with Currarino triad may also have associated spinal cord anomalies such as tethered cord, thickened filum terminale, or syrinx, which may be associated with urinary dysfunction. Diagnosis of Currarino triad is important, as correction of anorectal malformations is much more complex if associated with this entity (70).

In a recent case series of patients with Currarino triad, patients were diagnosed with imperforate anus, constipation, or pelvic abscess. The presacral masses in six out of 17 patients were pathologically confirmed as mature cystic teratomas, two of which were infected at clinical presentation. The remainder of cases were associated with lipomyelocele and lipomyelomeningocele. Anorectal malformations may range from relatively simple anorectal stenoses to imperforate anus or complex rectoperineal, rectovaginal, retrovestibular, or rectourethral fistulas (70).

CT images will demonstrate the presacral mass, which will appear cystic if it is a teratoma or meningocele (Fig 16a). CT will also demonstrate the sacral osseous defect, and three-dimensional reconstructions may aid in surgical planning. The sacral osseous defects may also be identified on pelvic radiographs (Fig 16b) (70). MRI is helpful in evaluating for communication between a cystic mass and the spinal canal. Anorectal malformations are best evaluated with contrast-material enema examination or at MRI (Fig 16c) (70).

Fetus in Fetu

Fetus in fetu is defined as a mass of tissue resembling a fetus located within a fully developed child or adult. There are two theories regarding the origin of fetus in fetu, namely that the mass represents either a highly developed teratoma or that the mass began as a normal fetus that was enveloped within its twin during the prenatal period. Fetus in fetu usually manifests with symptoms related to mass effect. The most common location of fetus in fetu is within the abdomen in the upper retroperitoneum. Other sites include the liver, cranium, pelvis, and neck. These masses typically derive arterial supply directly from the aorta and are managed with surgical excision (71,72).

The defining feature of fetus in fetu is the presence of an axial skeleton, which can be identified at radiography or CT (Fig 17). CT and US can further depict soft tissue, fluid, fat, and calcified components within the mass, although the ultrasound waves may be hampered by large

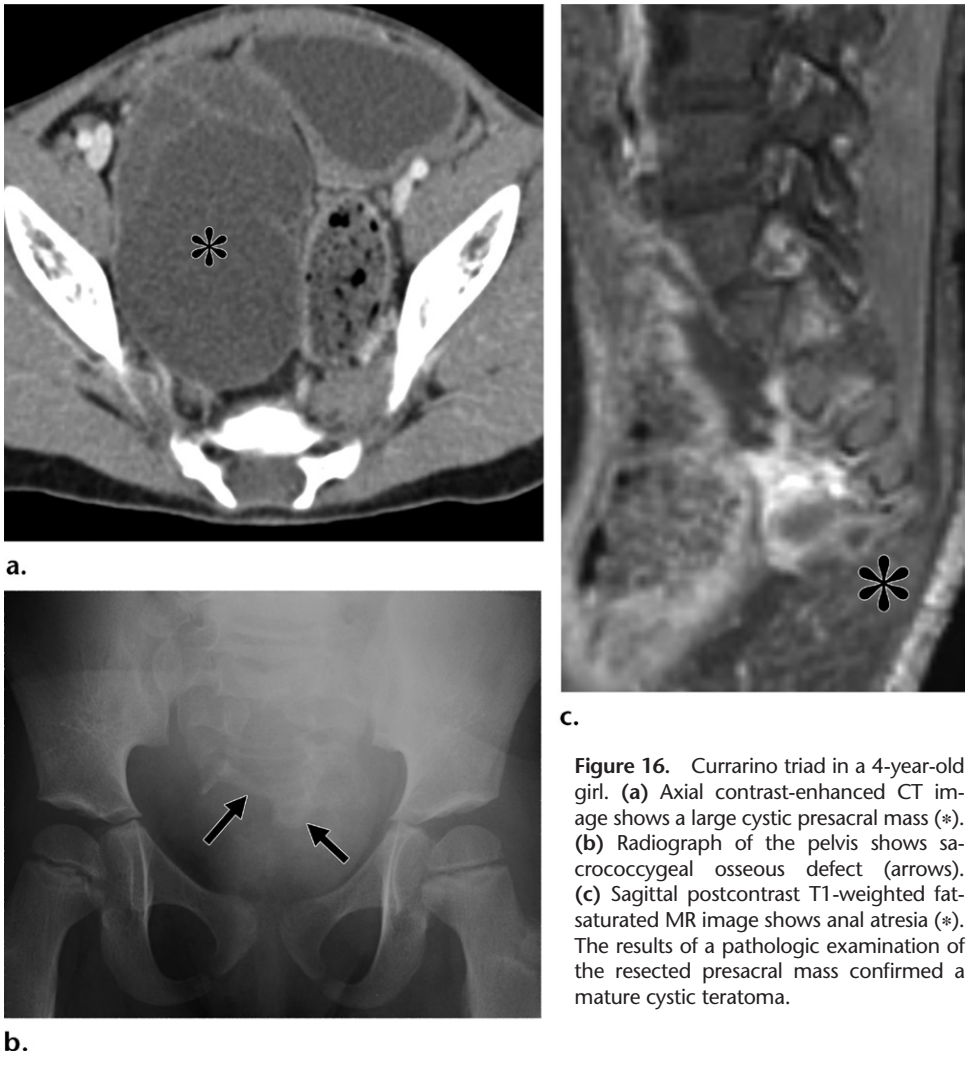

Figure 16. Currarino triad in a 4-year-old girl. **(a)** Axial contrast-enhanced CT image shows a large cystic presacral mass (*). **(b)** Radiograph of the pelvis shows sacrococcygeal osseous defect (arrows). **(c)** Sagittal postcontrast T1-weighted fat-saturated MR image shows anal atresia (*). The results of a pathologic examination of the resected presacral mass confirmed a mature cystic teratoma.

ossified structures. MRI may also be helpful in evaluation of this mass owing to excellent soft-tissue contrast enhancement, although MRI is not as helpful as CT in the evaluation of calcified structures. At excision, well-developed fetal organs are identified (71,72).

Pseudo-Meigs Syndrome

Meigs syndrome is the association of ascites, pleural effusion, and an ovarian fibroma. Pseudo-Meigs syndrome represents a variant of Meigs syndrome, with a nonfibromatous ovarian tumor. Various ovarian tumors have been reported to cause pseudo-Meigs syndrome, including metastases and ovarian teratomas. The pathogenesis of ascites in Meigs and pseudo-Meigs syndromes is possibly due to tumor compression of blood vessels and lymphatics leading to ascites. Other proposed causes for the ascites include direct transudation of fluid from the tumor surface, hormonal stimulation, or tumor torsion. Pleural effusion is thought to occur by the transfer of ascites through transdiaphragmatic lymphatic channels into the pleural space (73).

Typical imaging features of Meigs and pseudo-Meigs syndromes are ascites and pleural effusion, usually on the right with an associated ovarian lesion (73,74). Sampling of both peritoneal and pleural fluid will show identical composition for both, usually transudative (73). The presence of recurrent ascites and pleural effusion of unknown cause in an otherwise healthy woman should prompt an evaluation for an ovarian lesion at US.

Pancreatitis

Up to 4% of teratomas may contain mature pancreatic tissue (75). Although these are typically pancreatic endocrine elements, pancreatic tissue with exocrine function may be depicted (76,77). This mature pancreatic tissue may manifest with an elevated carbohydrate antigen 19–9 level or hypoglycemia (75,76,78,79). As with exocrine pancreas located elsewhere, pancreatic tissue located within a teratoma may develop pancreatitis and manifest with local pain (Fig 18). Imaging findings are nonspecific but may consist of adjacent fat stranding and fluid, which may mimic rupture or torsion.

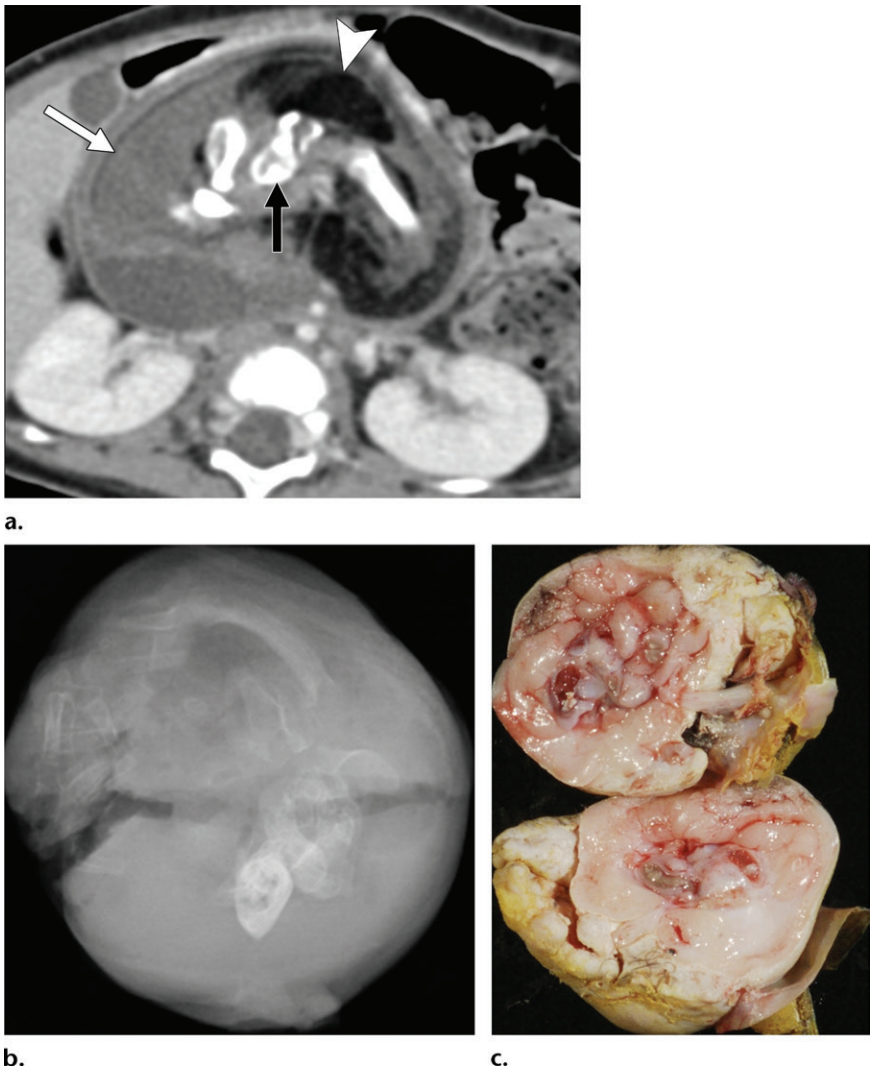

Figure 17. Fetus in fetu. **(a)** Axial contrast-enhanced CT image shows a mass containing soft tissue (white arrow), fat (arrowhead), and osseous elements (black arrow) in a fetuslike configuration. **(b)** Specimen radiograph of the excised mass shows osseous elements, a finding suggestive of a disorganized axial skeleton. **(c)** Gross photograph of the excised mass shows multiple tissue types in a fetuslike configuration.

Figure 18. Pancreatitis within a mediastinal teratoma in a 20-year-old woman presenting with right-sided chest pressure. Axial contrast-enhanced CT image shows a thick-walled cystic lesion (*) in the mediastinum. The results of a pathologic examination confirmed hemosiderin surrounding mature pancreatic elements, with patchy fat necrosis and infiltration by neutrophils, findings in keeping with pancreatitis within a teratoma.

Conclusion

Germ cell tumors can differentiate into a variety of tissue types and can exhibit unusual imaging characteristics. It is important to be aware of certain benign entities while evaluating for potential metastatic disease, including growing teratoma syndrome, ossified metastases, gliomatosis peritonei, sarcoidlike reaction, and ruptured dermoid cyst. Furthermore, a large soft-tissue component in a teratoma suggests either an immature teratoma, which usually manifests in younger patients, or a malignant transformation within a mature teratoma, which usually manifests in older patients. In addition, choriocarcinoma syndrome can lead to diffuse alveolar hemorrhage, subcapsular hematoma in the liver, and hemorrhagic shock. Finally, germ cell tumors may also be associated with rare endocrine and paraneoplastic syndromes.

References

1. Peterson CM, Buckley C, Holley S, Menias CO. Teratomas: a multimodality review. Curr Probl Diagn Radiol 2012;41(6):210–219.
2. Kaatsch P, Häfner C, Calaminus G, Blettner M, Tulla M. Pediatric germ cell tumors from 1987 to 2011: incidence rates, time trends, and survival. Pediatrics 2015;135(1):e136–e143.
3. Rusner C, Trabert B, Katalinic A, et al. Incidence patterns and trends of malignant gonadal and extragonadal germ cell tumors in Germany, 1998-2008. Cancer Epidemiol 2013;37(4):370–373.
4. Kühn MW, Weissbach L. Localization, incidence, diagnosis and treatment of extratesticular germ cell tumors. Urol Int 1985;40(3):166–172.
5. Ulbright TM. Germ cell tumors of the gonads: a selective review emphasizing problems in differential diagnosis, newly appreciated, and controversial issues. Mod Pathol 2005;18(suppl 2):S61–S79.
6. Kreydin EI, Barrisford GW, Feldman AS, Preston MA. Testicular cancer: what the radiologist needs to know. AJR Am J Roentgenol 2013;200(6):1215–1225.
7. Schmoll HJ, Jordan K, Huddart R, et al. Testicular seminoma: ESMO clinical practice guidelines for diagnosis, treatment and follow-up. Ann Oncol 2010;21(suppl 5):v140–v146.
8. Talerman A. Germ cell tumors of the ovary. In: Kurman, RJ, ed. Blaustein's pathology of the female genital tract. 5th ed. New York, NY: Springer, 2002; 1391.
9. Shinagare AB, Jagannathan JP, Ramaiya NH, Hall MN, Van den Abbeele AD. Adult extragonadal germ cell tumors. AJR Am J Roentgenol 2010;195(4):W274–W280.
10. Mortazavi N, Mahzooni P, Taheri D, Jalilian M, Novin K. Germ cell tumor's survival rate in young patients. Iran J Cancer Prev 2015;8(4):e3440.
11. Stang A, Trabert B, Wentzensen N, et al. Gonadal and extragonadal germ cell tumours in the United States: 1973-2007. Int J Androl 2012;35(4):616–625.
12. Arora RS, Alston RD, Eden TOB, Geraci M, Birch JM. Comparative incidence patterns and trends of gonadal and extragonadal germ cell tumors in England: 1979 to 2003. Cancer 2012;118(17):4290–4297.
13. Coursey Moreno C, Small WC, Camacho JC, et al. Testicular tumors: what radiologists need to know—differential diagnosis, staging, and management. RadioGraphics 2015;35(2):400–415.
14. Shaaban AM, Rezvani M, Elsayes KM, et al. Ovarian malignant germ cell tumors: cellular classification and clinical and imaging features. RadioGraphics 2014;34(3):777–801.
15. Frazier AL, Amatruda JF, eds. Pediatric germ cell tumors. New York, NY: Springer, 2014.
16. Sharma P, Jain TK, Parida GK, et al. Diagnostic accuracy of integrated (18)F-FDG PET/CT for restaging patients with malignant germ cell tumours. Br J Radiol 2014;87(1040):20140263.
17. Hart A, Vali R, Marie E, Shaikh F, Shammas A. The clinical impact of 18F-FDG PET/CT in extracranial pediatric germ cell tumors. Pediatr Radiol 2017;47(11):1508–1513.
18. Donohue JP, Zachary JM, Maynard BR. Distribution of nodal metastases in nonseminomatous testis cancer. J Urol 1982;128(2):315–320.
19. Xiao H, Liu D, Bajorin DF, Burt M, Bosl GW. Medical and surgical management of pulmonary metastases from germ cell tumors. Chest Surg Clin N Am 1998;8(1):131–143.
20. Denaro L, Pluchinotta F, Faggin R, et al. What's growing on? the growing teratoma syndrome. Acta Neurochir (Wien) 2010;152(11):1943–1946.
21. Aide N, Comoz F, Sevin E. Enlarging residual mass after treatment of a nonseminomatous germ cell tumor: growing teratoma syndrome or cancer recurrence? J Clin Oncol 2007;25(28):4494–4496.
22. Logothetis CJ, Samuels ML, Trindade A, Johnson DE. The growing teratoma syndrome. Cancer 1982;50(8): 1629–1635.
23. Gorbatiy V, Spiess PE, Pisters LL. The growing teratoma syndrome: current review of the literature. Indian J Urol 2009;25(2):186–189.
24. Han NY, Sung DJ, Park BJ, et al. Imaging features of growing teratoma syndrome following a malignant ovarian germ cell tumor. J Comput Assist Tomogr 2014;38(4):551–557.
25. Arana S, Fielli M, González A, Segovia J, Villaverde M. Choriocarcinoma syndrome in a 24-year-old male. JRSM Short Rep 2012;3(6):44.
26. Shintaku M, Hwang MH, Amitani R. Primary choriocarcinoma of the lung manifesting as diffuse alveolar hemorrhage. Arch Pathol Lab Med 2006;130(4):540–543.
27. Baagar K, Khan FY, Alkuwari E. Choriocarcinoma syndrome: a case report and a literature review. Case Rep Oncol Med 2013;2013:697251.
28. Aswani Y, Thakkar H, Hira P. Disseminated gestational choriocarcinoma presenting with hepatic and uveal metastases, hook effect, and choriocarcinoma syndrome. Indian J Radiol Imaging 2016;26(4):482–486.
29. Kandori S, Kawai K, Fukuhara Y, et al. A case of metastatic testicular cancer complicated by pulmonary hemorrhage due to choriocarcinoma syndrome. Int J Clin Oncol 2010;15(6):611–614.
30. McKendrick JJ, Theaker J, Mead GM. Nonseminomatous germ cell tumor with very high serum human chorionic gonadotropin. Cancer 1991;67(3):684–689.
31. Seo JB, Im JG, Goo JM, Chung MJ, Kim MY. Atypical pulmonary metastases: spectrum of radiologic findings. RadioGraphics 2001;21(2):403–417.
32. Liang L, Zhang Y, Malpica A, et al. Gliomatosis peritonei: a clinicopathologic and immunohistochemical study of 21 cases. Mod Pathol 2015;28(12):1613–1620.
33. Shefren G, Collin J, Soriero O. Gliomatosis peritonei with malignant transformation: a case report and review of the literature. Am J Obstet Gynecol 1991;164(6 Pt 1):1617–1620; discussion 1620–1621.
34. Tchernev G, Tana C, Schiavone C, Cardoso JC, Ananiev J, Wollina U. Sarcoidosis vs. sarcoid-like reactions: the two sides of the same coin? Wien Med Wochenschr 2014;164(13-14):247–259.
35. Chowdhury FU, Sheerin F, Bradley KM, Gleeson FV. Sarcoid-like reaction to malignancy on whole-body integrated (18)F-FDG PET/CT: prevalence and disease pattern. Clin Radiol 2009;64(7):675–681.
36. Kaikani W, Boyle H, Chatte G, et al. Sarcoid-like granulomatosis and testicular germ cell tumor: the 'great imitator.' Oncology 2011;81(5-6):319–324.
37. Miller BH, Rosado-de-Christenson ML, McAdams HP, Fishback NF. Thoracic sarcoidosis: radiologic-pathologic correlation. RadioGraphics 1995;15(2):421–437.
38. Targonska B, Frost J, Prabhu S. Anti-Ma2-antibody-associated encephalitis: an atypical paraneoplastic neurologic syndrome. S Afr J Rad 2018;22(1):a1310.
39. Dalmau J, Rosenfeld MR. Paraneoplastic syndromes of the CNS. Lancet Neurol 2008;7(4):327–340.
40. Kelley BP, Patel SC, Marin HL, Corrigan JJ, Mitsias PD, Griffith B. Autoimmune encephalitis: pathophysiology and imaging review of an overlooked diagnosis. AJNR Am J Neuroradiol 2017;38(6):1070–1078.
41. Azizyan A, Albrektson JR, Maya MM, Pressman BD, Moser F. Anti-NMDA encephalitis: an uncommon, autoimmune mediated form of encephalitis. J Radiol Case Rep 2014;8(8):1–6.
42. Kim I, Lee JY, Kwon JH, et al. A case of autoimmune hemolytic anemia associated with an ovarian teratoma. J Korean Med Sci 2006;21(2):365–367.
43. Gilligan TD, Seidenfeld J, Basch EM, et al. American Society of Clinical Oncology Clinical Practice Guideline on uses of serum tumor markers in adult males with germ cell tumors. J Clin Oncol 2010;28(20):3388–3404.
44. Bjurlin MA, August CZ, Weldon-Linne M, Totonchi E. Histologically pure stage I seminoma with an elevated β-hCG of 4497 IU/l. Urology 2007;70(5):1007.e13–1007.e15.
45. Parkinson CA, Hatcher HM, Ajithkumar TV. Management of malignant ovarian germ cell tumors. Obstet Gynecol Surv 2011;66(8):507–514.
46. Downey GP, Prentice M, Penna LK, Gleeson RP, Elder MG. Ectopic beta-human chorionic gonadotropin production by a dermoid cyst. Am J Obstet Gynecol 1989;160(2): 449–451.

47. Englund AT, Geffner ME, Nagel RA, Lippe BM, Braunstein GD. Pediatric germ cell and human chorionic gonadotropin-producing tumors: clinical and laboratory features. Am J Dis Child 1991;145(11):1294–1297.
48. Rahmani S, Turton P, Shaaban A, Dall B. Overview of gynecomastia in the modern era and the Leeds Gynaecomastia Investigation algorithm. Breast J 2011;17(3):246–255.
49. Yoshimura M, Hershman JM. Thyrotropic action of human chorionic gonadotropin. Thyroid 1995;5(5):425–434.
50. Woodruff JD, Rauh JT, Markley RL. Ovarian struma. Obstet Gynecol 1966;27(2):194–201.
51. Robboy SJ, Scully RE. Strumal carcinoid of the ovary: an analysis of 50 cases of a distinctive tumor composed of thyroid tissue and carcinoid. Cancer 1980;46(9):2019–2034.
52. Kostoglou-Athanassiou I, Lekka-Katsouli I, Gogou L, Papagrigoriou L, Chatonides I, Kaldrymides P. Malignant struma ovarii: report of a case and review of the literature. Horm Res 2002;58(1):34–38.
53. DeSimone CP, Lele SM, Modesitt SC. Malignant struma ovarii: a case report and analysis of cases reported in the literature with focus on survival and I^{131} therapy. Gynecol Oncol 2003;89(3):543–548.
54. Fibus TF. Intraperitoneal rupture of a benign cystic ovarian teratoma: findings at CT and MR imaging. AJR Am J Roentgenol 2000;174(1):261–262.
55. Rha SE, Byun JY, Jung SE, et al. CT and MR imaging features of adnexal torsion. RadioGraphics 2002;22(2): 283–294.
56. Pantoja E, Noy MA, Axtmayer RW, Colon FE, Pelegrina I. Ovarian dermoids and their complication: comprehensive historical review. Obstet Gynecol Surv 1975;30(1):1–20.
57. Madhusudhan KS, Sharma R, Gadodia A, Kumar A. Spontaneous rupture of benign mediastinal teratoma: a report of two cases. Indian J Med Paediatr Oncol 2012;33(2):123–125.
58. Choi SJ, Lee JS, Song KS, Lim TH. Mediastinal teratoma: CT differentiation of ruptured and unruptured tumors. AJR Am J Roentgenol 1998;171(3):591–594.
59. Machuca JS, Tejwani D, Niazi M, Diaz-Fuentes G. A large ruptured mediastinal cystic teratoma. J Bronchology Interv Pulmonol 2010;17(3):269–272.
60. Serraj M, Lakranbi M, Ghalimi J, Ouadnouni Y, Smahi M. Mediastinal mature teratoma with complex rupture into the lung, bronchus and skin: a case report. World J Surg Oncol 2013;11(1):125.
61. Escalon JG, Arkin J, Chaump M, Harkin TJ, Wolf AS, Legasto A. Ruptured anterior mediastinal teratoma with radiologic, pathologic, and bronchoscopic correlation. Clin Imaging 2015;39(4):689–691.
62. Bell C, Domingo F, Miller AD, Smith JS, Headrick JR Jr. Traumatic rupture of a posterior mediastinal teratoma following motor-vehicle accident. Case Rep Surg 2016;2016:7172062.
63. Ray MJ, Barnett DW, Snipes GJ, Layton KF, Opatowsky MJ. Ruptured intracranial dermoid cyst. Proc Bayl Univ Med Cent 2012;25(1):23–25.
64. Peterson WF. Malignant degeneration of benign cystic teratomas of the overy: a collective review of the literature. Obstet Gynecol Surv 1957;12(6):793–830.
65. Kikkawa F, Ishikawa H, Tamakoshi K, Nawa A, Suganuma N, Tomoda Y. Squamous cell carcinoma arising from mature cystic teratoma of the ovary: a clinicopathologic analysis. Obstet Gynecol 1997;89(6):1017–1022.
66. Arioz DT, Tokyol C, Sahin FK, et al. Squamous cell carcinoma arising in a mature cystic teratoma of the ovary in young patient with elevated carbohydrate antigen 19-9. Eur J Gynaecol Oncol 2008;29(3):282–284.
67. Yokoyama T, Takehara K, Yamamoto Y, et al. The usefulness of 18F-FDG-PET/CT in discriminating benign from malignant ovarian teratomas. Int J Clin Oncol 2015;20(5):960–966.
68. Mohapatra T, Arora A, Srikant K, Snehalata, Kumar N. A rare case of mature teratoma: has FDG PET/CT a role to play? Indian J Nucl Med 2011;26(2):107–108.
69. Currarino G, Coln D, Votteler T. Triad of anorectal, sacral, and presacral anomalies. AJR Am J Roentgenol 1981;137(2):395–398.
70. AbouZeid AA, Mohammad SA, Abolfotoh M, Radwan AB, Ismail MME, Hassan TA. The Currarino triad: what pediatric surgeons need to know. J Pediatr Surg 2017;52(8):1260–1268.
71. Gupta SK, Singhal P, Arya N. Fetus-in-fetu: a rare congenital anomaly. J Surg Tech Case Rep 2010;2(2):77–80.
72. Saito K, Katsumata Y, Hirabuki T, Kato K, Yamanaka M. Fetus-in-fetu: parasite or neoplasm?—a study of two cases. Fetal Diagn Ther 2007;22(5):383–388.
73. Kazanov L, Ander DS, Enriquez E, Jaggi FM. Pseudo-Meigs' syndrome. Am J Emerg Med 1998;16(4):404–405.
74. Yamamoto Y, Miyagawa Y, Ehara T, et al. Three cases of pseudo-Meigs' syndrome secondary to ovarian metastases from colorectal cancer. Case Rep Surg 2017;2017:5235368.
75. Suda K, Mizuguchi K, Hebisawa A, Wakabayashi T, Saito S. Pancreatic tissue in teratoma. Arch Pathol Lab Med 1984;108(10):835–837.
76. Agrawal T, Blau AJ, Chwals WJ, Tischler AS. A unique case of mediastinal teratoma with mature pancreatic tissue, nesidioblastosis, and aberrant islet differentiation: a case report and literature review. Endocr Pathol 2016;27(1):21–24.
77. Audet IM, Goldhahn RT Jr, Dent TL. Adult sacrococcygeal teratomas. Am Surg 2000;66(1):61–65.
78. Minami H, Itoyanagi N, Kubota F, Nakamura Y. A case of mediastinal mature teratoma presenting increased serum CA19-9 level [in Japanese]. Nihon Kyobu Geka Gakkai Zasshi 1994;42(11):2139–2143.
79. Uygur-Bayramicli O, Dabak R, Orbay E, et al. Type 2 diabetes mellitus and CA 19-9 levels. World J Gastroenterol 2007;13(40):5357–5359.